

Numerical investigation of spatiotemporal chaos in nonlinear lattice models

Haris Skokos

**Department of Mathematics and Applied Mathematics
University of Cape Town
Cape Town, South Africa**

**E-mail: haris.skokos@uct.ac.za
URL: http://math_research.uct.ac.za/~hskokos/**

International Conference on Στατιστική Φυσική, 11 July 2023, Crete, Greece

University of Cape Town (UCT)



Outline

- **The one-dimensional quartic disordered Klein-Gordon (1D DKG) model: Different dynamical regimes**
- **Maximum Lyapunov Exponent (MLE): strength of chaos**
- **Deviation Vector Distributions (DVDs): mechanisms of chaotic spreading**
- **Frequency Map Analysis (FMA): characteristics of spatiotemporal evolution of chaos**
- **Generalized Alignment Index (GALI): localized vs. spreading chaos**
- **Summary**

The one-dimensional disordered Klein Gordon model (1D DKG)

$$H = \sum_{l=1}^N \frac{p_l^2}{2} + \frac{\tilde{\epsilon}_l}{2} u_l^2 + \frac{1}{4} u_l^4 + \frac{1}{2W} (u_{l+1} - u_l)^2$$

with **fixed boundary conditions** $u_0=p_0=u_{N+1}=p_{N+1}=0$. Typically $N=1000$.

Parameters: W and the **total energy** H . $\tilde{\epsilon}_l$ chosen uniformly from $\left[\frac{1}{2}, \frac{3}{2}\right]$.

Linear case (neglecting the term $u_l^4/4$)

Ansatz: $u_l = A_l \exp(i\omega t)$. **Normal modes (NMs) $A_{v,l}$ - Eigenvalue problem:**

$$\lambda A_l = \epsilon_l A_l - (A_{l+1} + A_{l-1}) \text{ with } \lambda = W\omega^2 - W - 2, \quad \epsilon_l = W(\tilde{\epsilon}_l - 1)$$

Anderson localization [Anderson, Phys. Rev. (1958)]. Experiments on BEC [Billy et al., Nature (2008)]

What happens in the presence of nonlinearity?

Will nonlinearity destroy localization?

Characteristics of energy distributions

We consider normalized **energy distributions** $\xi_l = \frac{H_l}{\sum_m H_m}$

with $H_l = \frac{p_l^2}{2} + \frac{\tilde{\epsilon}_l}{2} u_l^2 + \frac{1}{4} u_l^4 + \frac{1}{4W} (u_{l+1} - u_l)^2$

Second moment: $m_2 = \sum_{l=1}^N (l - \bar{l})^2 \xi_l$ with $\bar{l} = \sum_{l=1}^N l \xi_l$

Participation number: $P = \frac{1}{\sum_{l=1}^N \xi_l^2}$

measures the number of stronger excited sites in ξ_l .

Single site $P=1$. Equipartition of energy $P=N$.

Different dynamical regimes

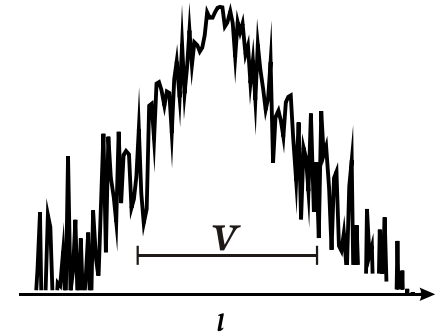
Three expected evolution regimes [Flach, Chem. Phys (2010) - S. & Flach, PRE (2010) - Lapyteva et al., EPL (2010) - Bodyfelt et al., PRE (2011)]

Δ : width of the frequency spectrum. $\Delta = 1 + \frac{4}{W}$ since $\omega_v^2 \in \left[\frac{1}{2}, \frac{3}{2} + \frac{4}{W}\right]$

d : average spacing of interacting modes. $d \approx \frac{\Delta}{V}$,

V : localization volume of an eigenstate $V \sim \frac{1}{\sum_{l=1}^N A_{v,l}^4}$

δ : nonlinear frequency shift. $\delta_l = \frac{3H_l}{2\tilde{\epsilon}_l} \propto H$



Weak Chaos Regime: $\delta < d$, $m_2 \propto t^{1/3}$ ($P \propto t^{1/6}$)

Frequency shift is less than the average spacing of interacting modes. NMs are weakly interacting with each other. [Molina, PRB (1998) – Pikovsky & Shepelyansky, PRL (2008) – Flach et al., PRL (2009)].

Strong Chaos Regime: $d < \delta < \Delta$, $m_2 \propto t^{1/2}$ ($P \propto t^{1/4}$) $\rightarrow m_2 \propto t^{1/3}$

Almost all NMs in the packet are resonantly interacting. Wave packets initially spread faster and eventually enter the weak chaos regime.

Selftrapping Regime: $\delta > \Delta$

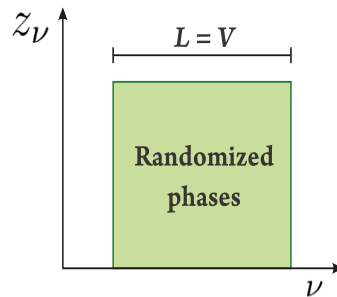
Frequency shift exceeds the spectrum width. Frequencies of excited NMs are tuned out of resonances with the nonexcited ones, leading to selftrapping, while a small part of the wave packet subdiffuses [Kopidakis et al., PRL (2008)].

Strong and weak chaos regimes

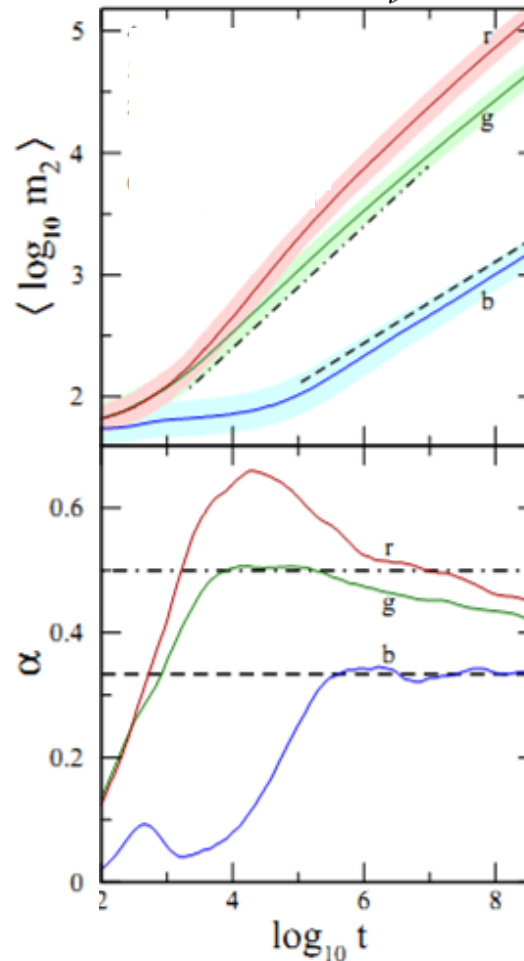
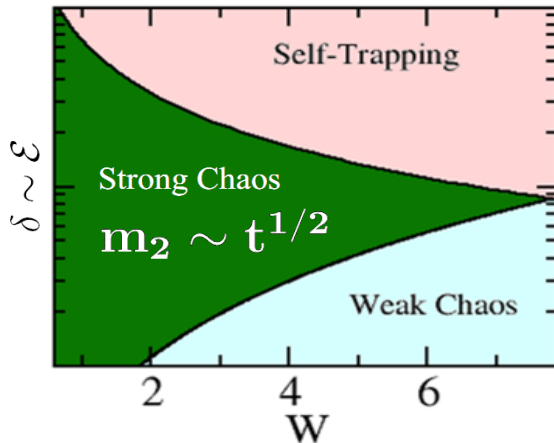
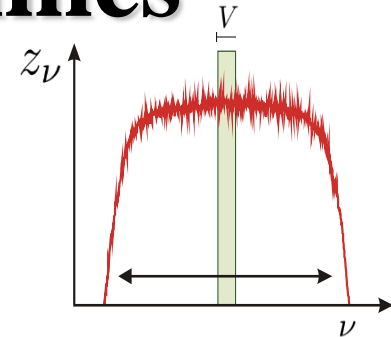
We consider **compact initial wave packets of width L**

[Laptyeva et al., EPL (2010)

– Bodyfelt et al., PRE (2011)]



Time evolution



$H = 0.01, 0.2, 0.75$

$W=4$

Average over 1000 realizations!

$\alpha=1/2$

$\alpha=1/3$

$$\alpha(\log t) = \frac{d\langle \log m_2 \rangle}{d \log t}$$

Maximum Lyapunov Exponent (MLE)

Chaos: sensitive dependence on initial conditions.

Roughly speaking, the MLE of a given orbit characterizes the **mean exponential rate of divergence** of trajectories surrounding it.

Consider an orbit in the $2N$ -dimensional phase space with **initial condition $\mathbf{x}(0)$** and **an initial deviation vector (small perturbation) from it $\mathbf{v}(0)$** .

Then the mean exponential rate of divergence is:

$$\text{MLE} = \lambda_1 = \lim_{t \rightarrow \infty} \Lambda(t) = \lim_{t \rightarrow \infty} \frac{1}{t} \ln \frac{\|\mathbf{v}(t)\|}{\|\mathbf{v}(0)\|}$$

$\lambda_1 = 0 \rightarrow$ Regular motion ($\Lambda \propto t^{-1}$)

$\lambda_1 > 0 \rightarrow$ Chaotic motion

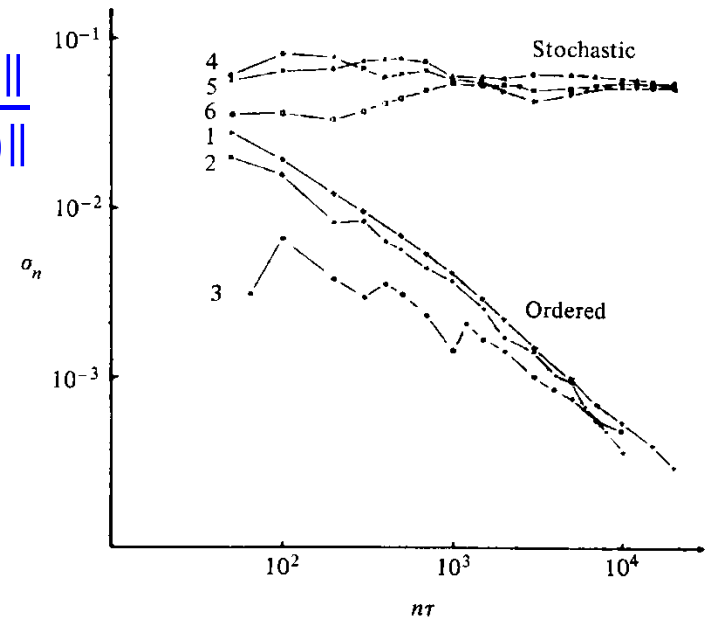
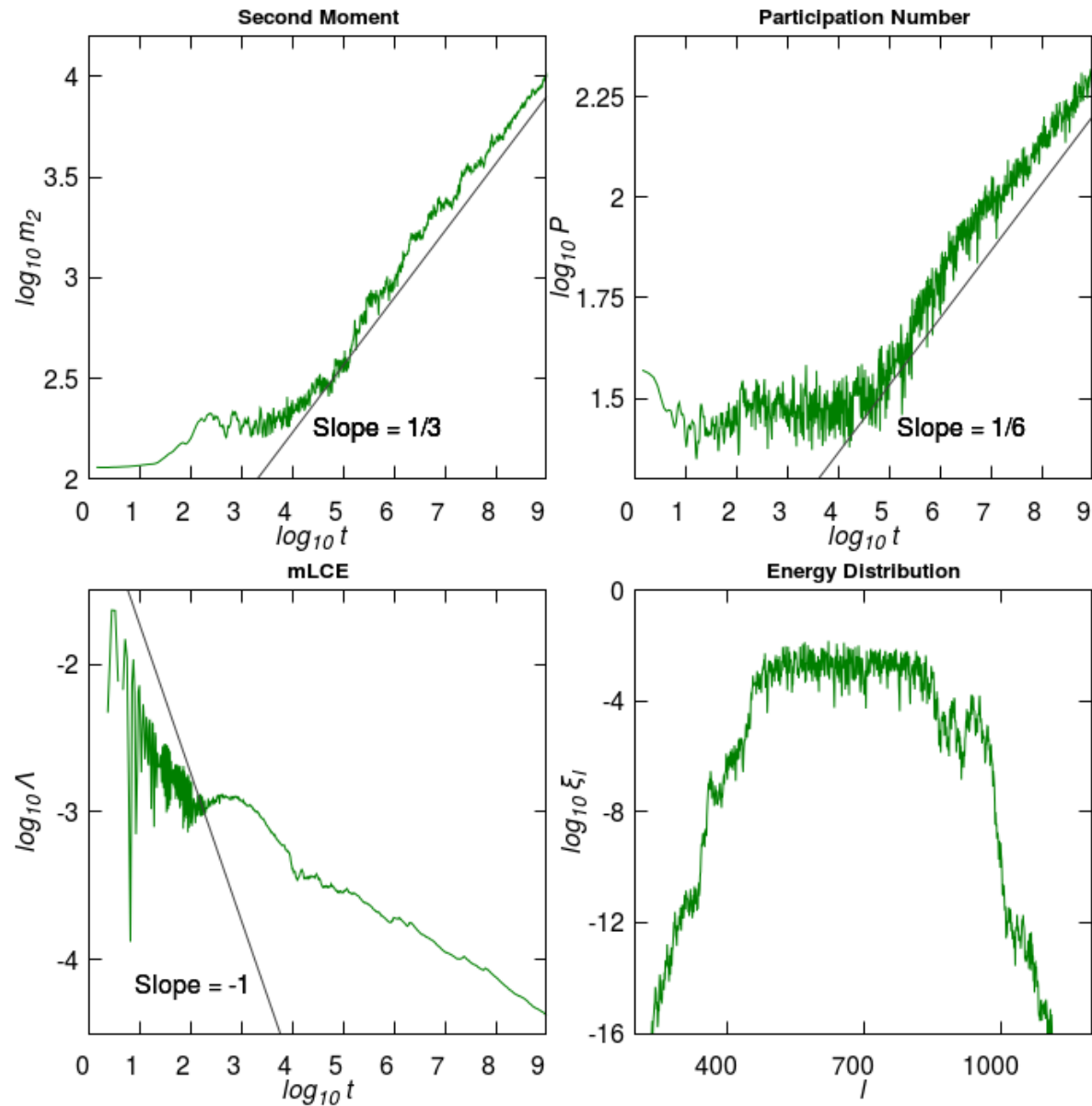


Figure 5.7. Behavior of σ_n at the intermediate energy $E = 0.125$ for initial points taken in the ordered (curves 1–3) or stochastic (curves 4–6) regions (after Benettin *et al.*, 1976).

A weak chaos case

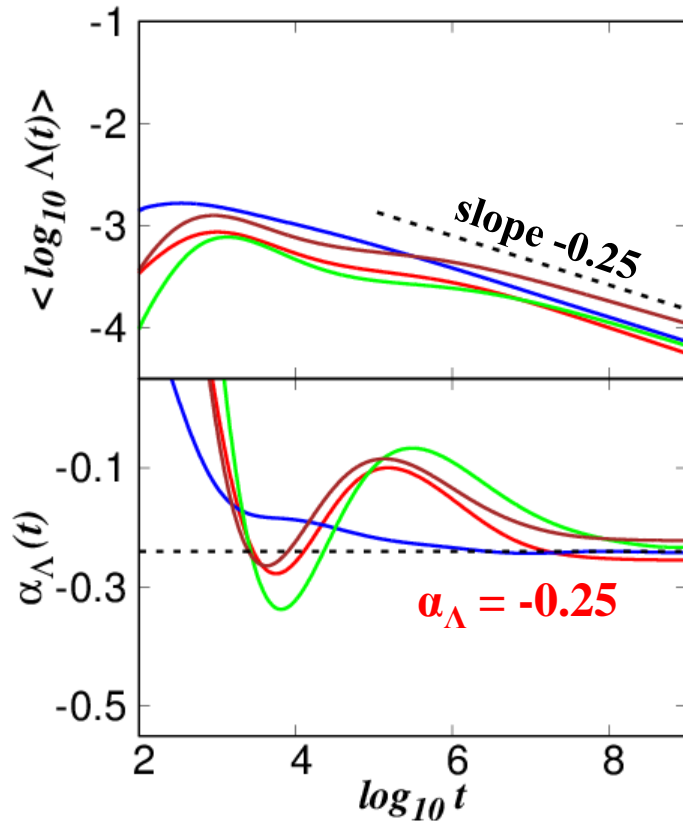
Block excitation
 $L=37$ sites,
 $H=0.37$, $W=3$.

One disorder
realization

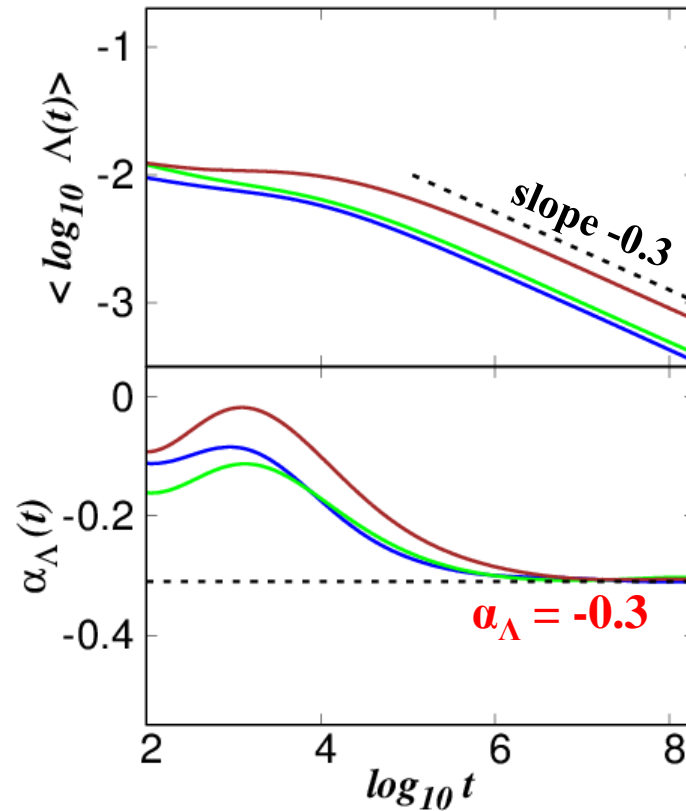


Time evolution of the MLE: $\Lambda \propto t^{\alpha_\Lambda}$

**Weak
chaos**



**Strong
chaos**



Average over 100 realizations [Senyange et al., PRE (2018)]

Block excitation (L=37 sites) H=0.37, W=3

Single site excitation H=0.4, W=4

Block excitation (L=21 sites) H=0.21, W=4

Block excitation (L=13 sites) H=0.26, W=5

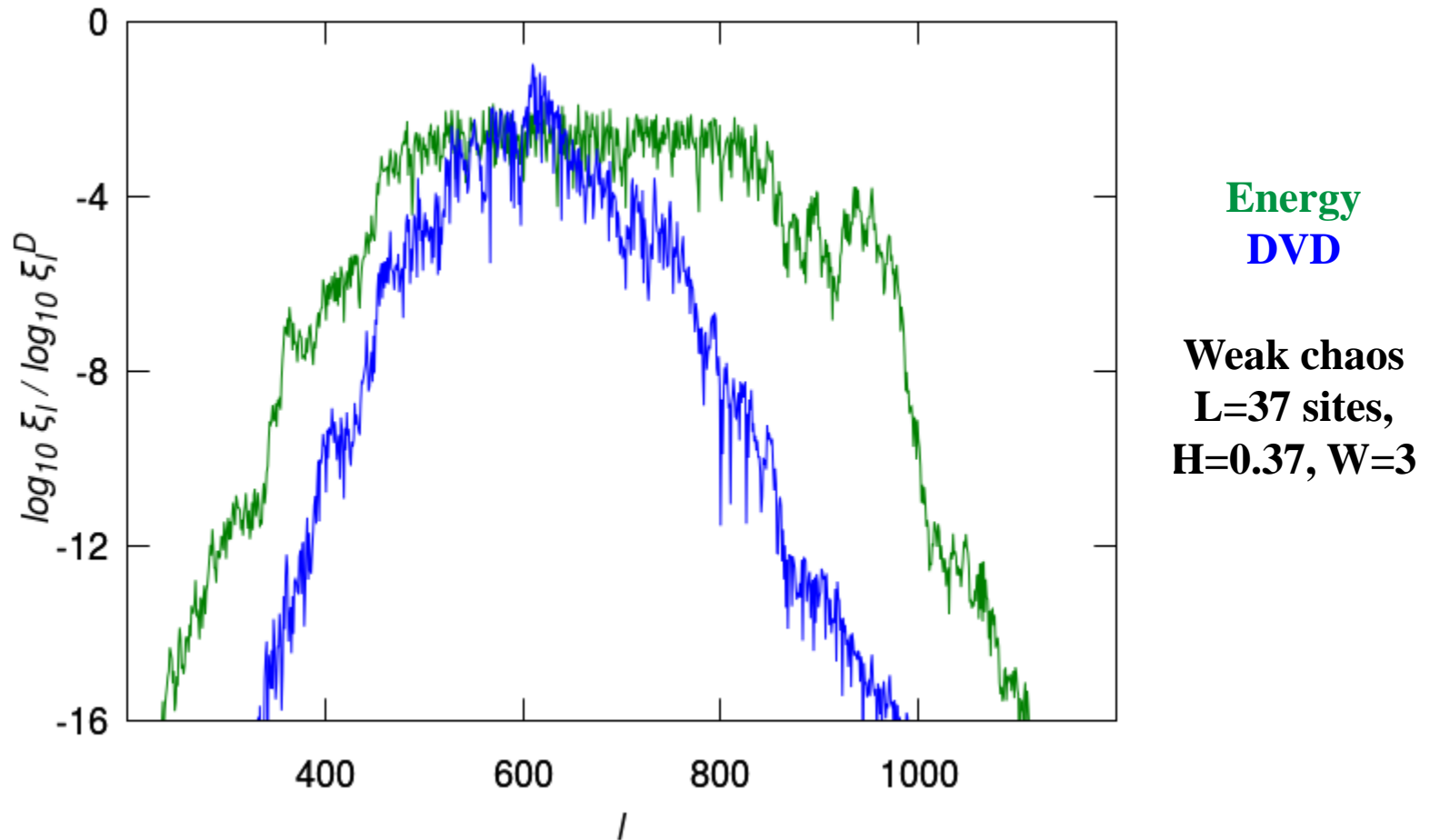
Block excitation (L=83 sites) H=0.83, W=2

Block excitation (L=37 sites) H=0.37, W=3

Block excitation (L=83 sites) H=0.83, W=3

The weak chaos case was also studied in S. et al., PRL (2013)

Deviation Vector Distributions (DVDs)



Deviation vector:

$$\mathbf{v}(t) = (\delta u_1(t), \delta u_2(t), \dots, \delta u_N(t), \delta p_1(t), \delta p_2(t), \dots, \delta p_N(t))$$

$$\text{DVD: } \xi_l^D = \frac{\delta u_l^2 + \delta p_l^2}{\sum_l (\delta u_l^2 + \delta p_l^2)}$$

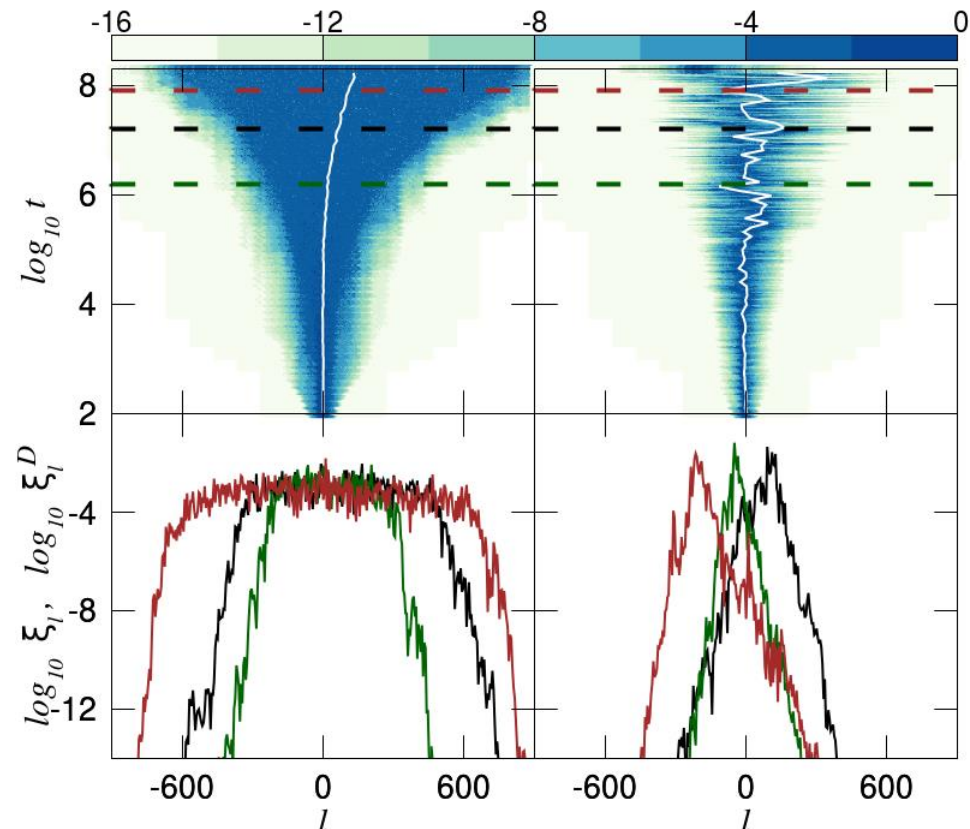
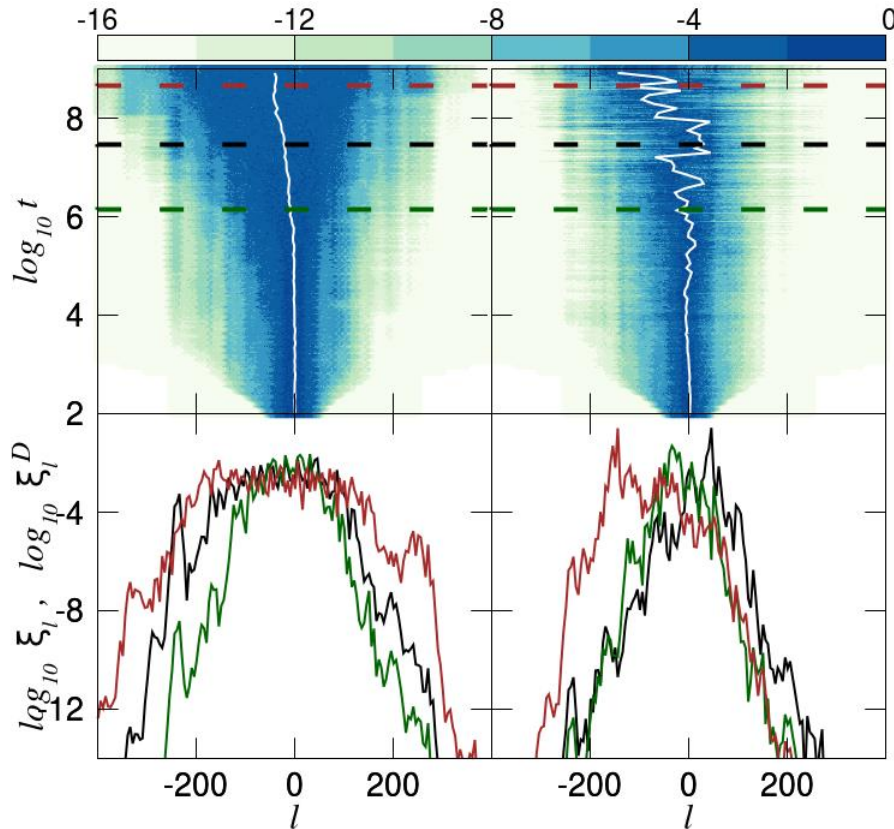
DVDs: Weak and Strong Chaos

Weak chaos

Strong chaos

Energy DVD

Energy DVD



$W=3, L=37, H=0.37$

$W=3, L=83, H=8.3$

Chaotic hot spots meander through the system, supporting the homogeneity of chaos inside the wave packet. A rather small number of sites are highly chaotic at each time.

Frequency Map Analysis (FMA)

Compute the **fundamental frequencies**, f_1 and f_2 , of an observable related to the evolution of an orbit in **two successive time windows** of the same length, and check **whether or not these frequencies change in time** [Laskar, Icarus (1990) – Laskar et al., Physica D (1992) – Laskar, Physica D (1993) – Robutel & Laskar, Icarus (2000)].

Regular motion: The computed frequencies do not vary in time

Chaotic motion: The computed frequencies vary in time

For every lattice site l we compute the fundamental frequencies f_{1l} and f_{2l} for time windows of length $T = 6 \cdot 10^5$ time units and evaluate the **relative change** of these two frequencies:

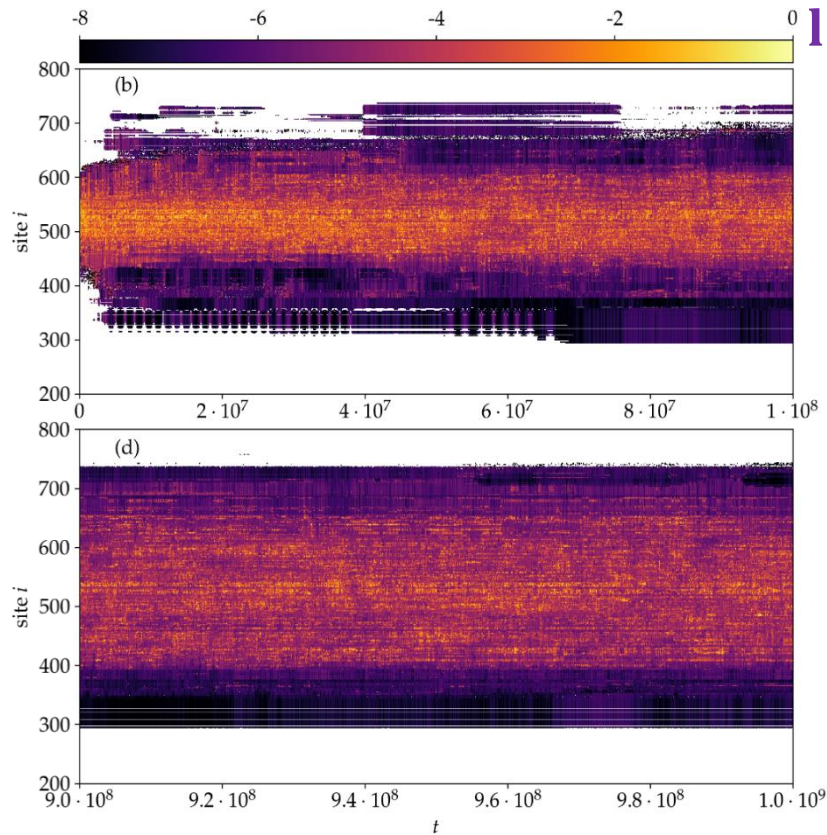
$$D_l = \left| \frac{f_{2l} - f_{1l}}{f_{1l}} \right|$$

Regular motion: small D_l values

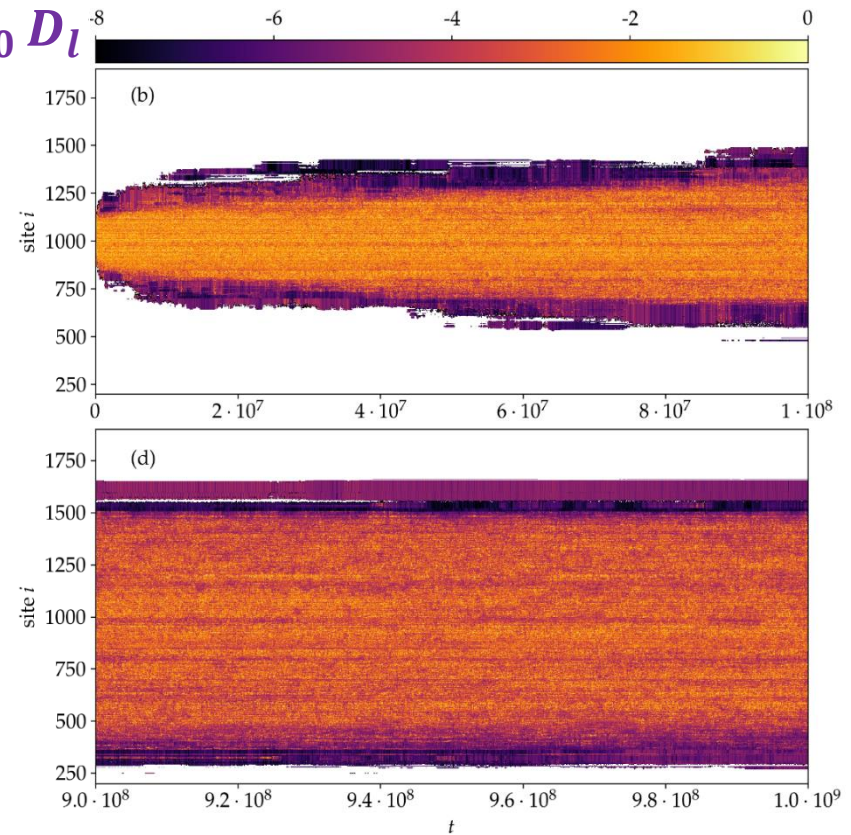
Chaotic motion: large D_l values

FMA: Weak and Strong Chaos

Weak chaos
 $L=1, H=0.4, W=4, N=999$



Strong chaos
 $L=21, H=4.2, W=4, N=3499$



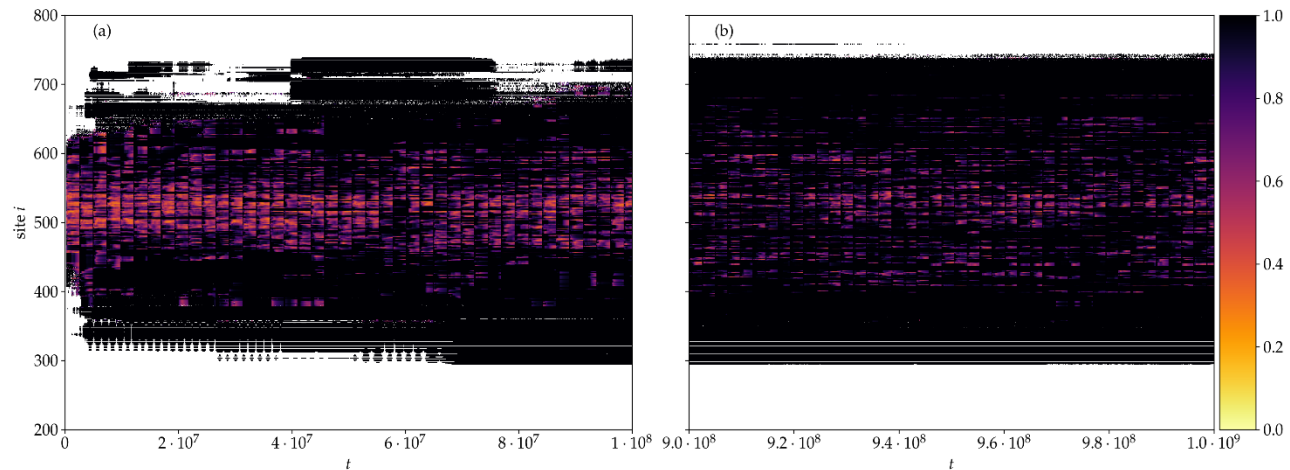
Chaotic behavior appears at the central regions of the wave packet, where the energy density is relatively large. The chaotic component of the wave packet **is more extended in the strong chaos case** [S. et al., IJBC (2022)]

Frequency Locking (FL)

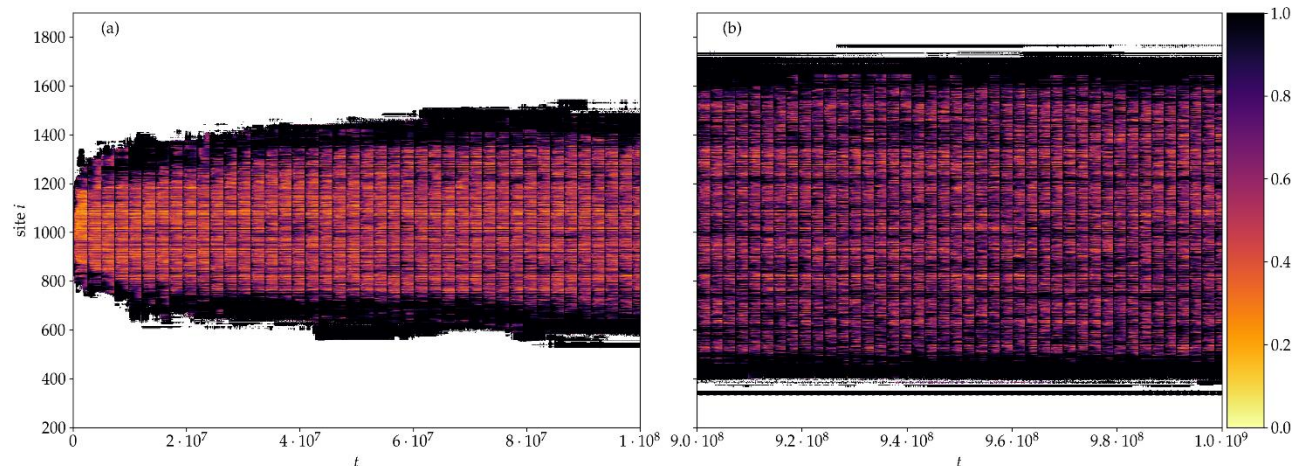
Frequency bins of width 10^{-4} . For each lattice site and a duration of $t = 2.4 \cdot 10^7$ we compute the fundamental frequencies in 200 time windows and register the related bins.

FL_i : the fraction of the most visited bin ($0 \leq FL_i \leq 1$). Measures the degree of practical frequency constancy (denoting nonchaotic behavior) of each oscillator.

Weak chaos



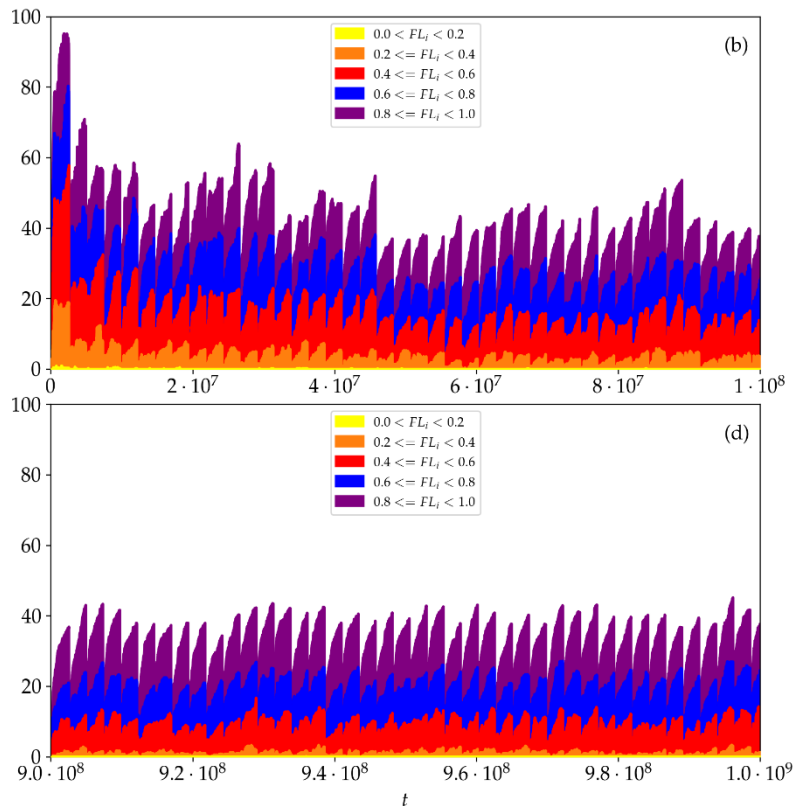
Strong chaos



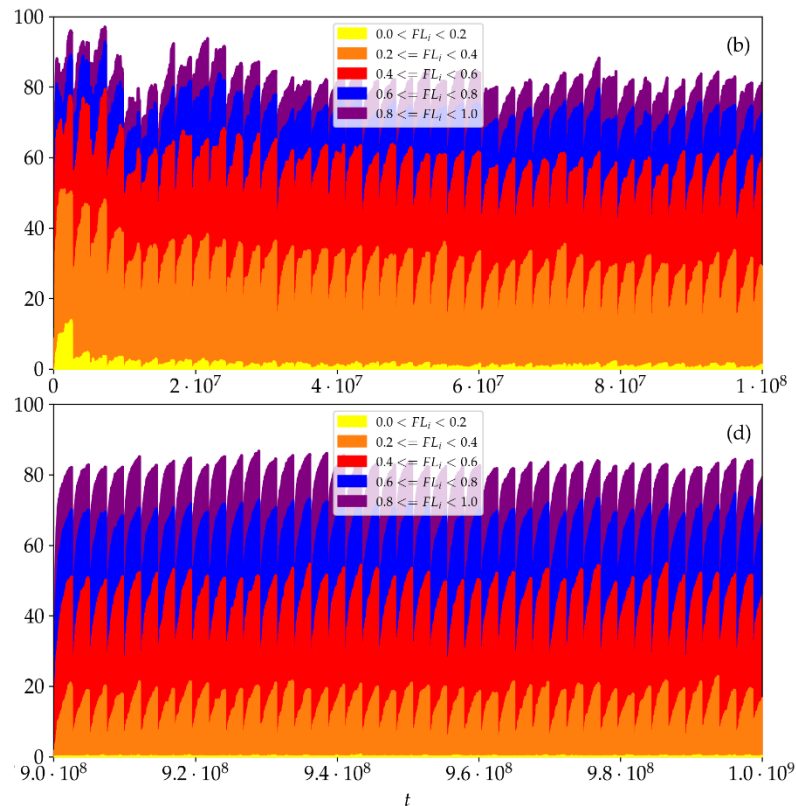
Frequency Locking (FL)

Accumulated percentages P_{FL} of sites with values in a particular FL range

Weak chaos



Strong chaos



The fraction of **sites behaving chaotically** is much larger in the strong chaos regime.

The percentage of **strongly chaotic sites (having $FL_i < 0.4$)** is about 5 times larger for strong chaos.

For **both spreading regimes**, the fraction of **highly chaotic oscillators ($FL_i < 0.4$) decreases in time**, although the percentage of chaotic sites remains practically constant.

The Generalized Alignment Index (GALI)

In the case of an N degree of freedom Hamiltonian system or a $2N$ symplectic map we follow the evolution of

k deviation vectors with $2 \leq k \leq 2N$,

and define [S. et al., Physica D, (2007)] the Generalized Alignment Index (GALI) of order k :

$$GALI_k(t) = \|\hat{v}_1(t) \wedge \hat{v}_2(t) \wedge \dots \wedge \hat{v}_k(t)\|$$

where

$$\hat{v}_1(t) = \frac{v_1(t)}{\|v_1(t)\|}.$$

$GALI_k$ is defined as the volume of the parallelepiped formed by the k normalized deviation vectors

Behavior of the $GALI_k$

Chaotic motion: $GALI_k$ ($2 \leq k \leq 2N$) tends exponentially to zero with exponents which involve the values of the first k largest Lyapunov exponents $\lambda_1, \lambda_2, \dots, \lambda_k$:

$$GALI_k(t) \propto e^{-[(\lambda_1 - \lambda_2) + (\lambda_1 - \lambda_3) + \dots + (\lambda_1 - \lambda_k)]t}$$

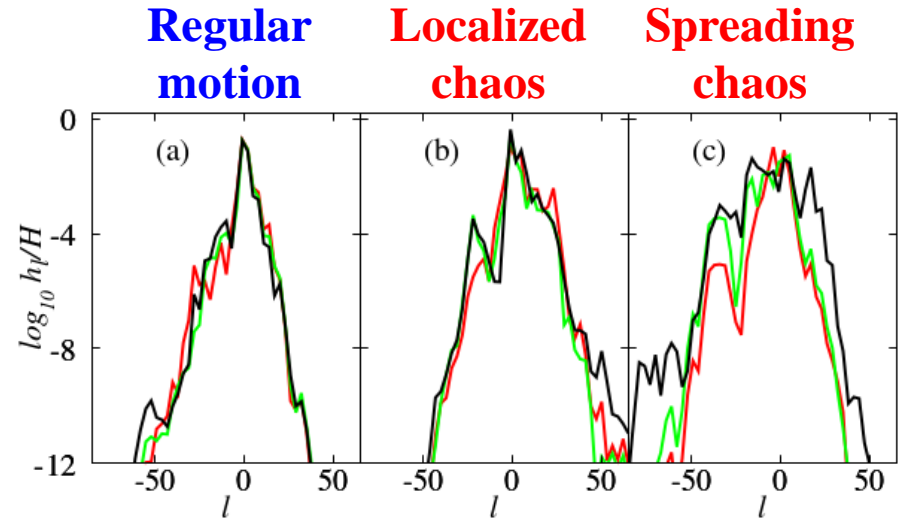
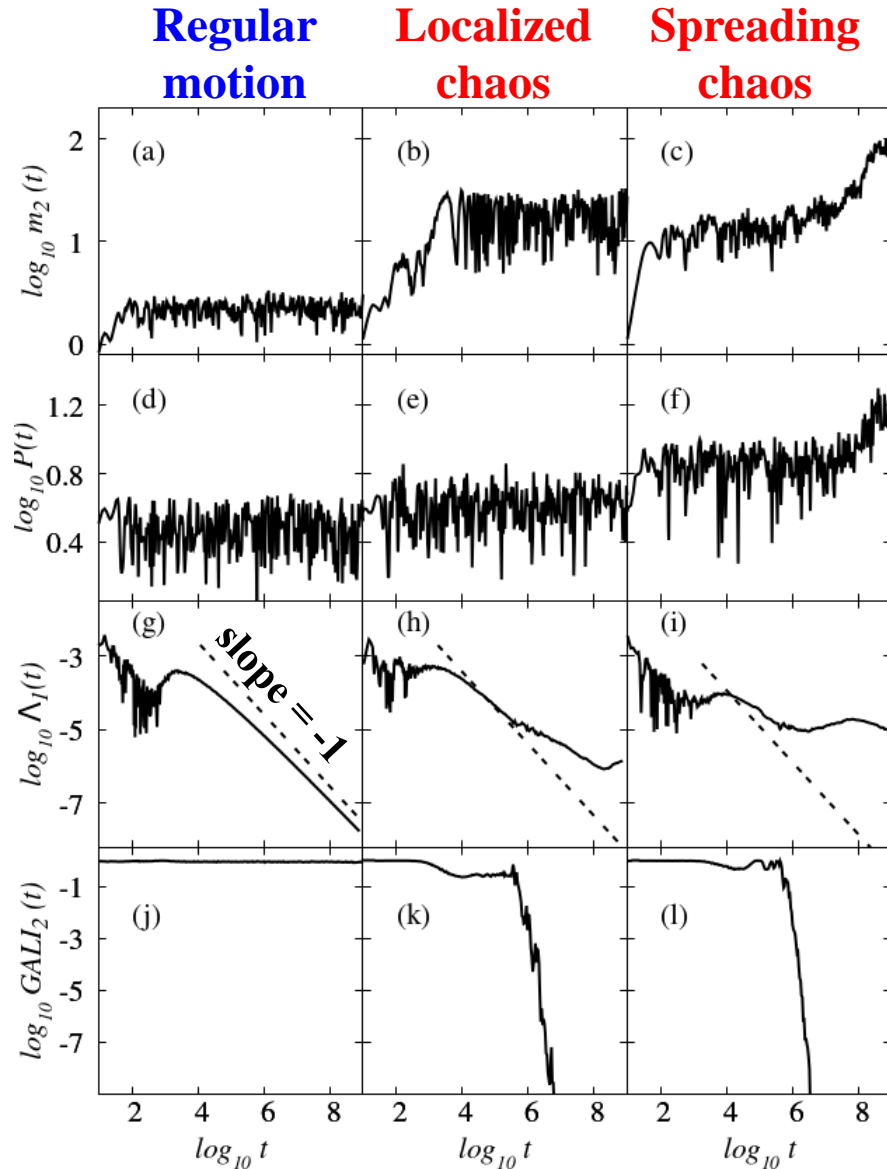
Regular motion: When the motion occurs on an N -dimensional torus then the behavior of $GALI_k$ is given by [S. et al., Eur. Phys. J. Sp. Top. (2008)]:

$$GALI_k(t) \propto \begin{cases} \text{constant} & \text{if } 2 \leq k \leq N \\ \frac{1}{t^{2(k-N)}} & \text{if } N < k \leq 2N \end{cases}$$

Here we only consider $GALI_2$ ($k=2$) which is equivalent to the **Smaller Alignment Index (SALI)** [S, J. Phys A (2001)].

Regular vs. chaotic (localized or spreading) motion

Different disorder realizations can exhibit different behaviors.



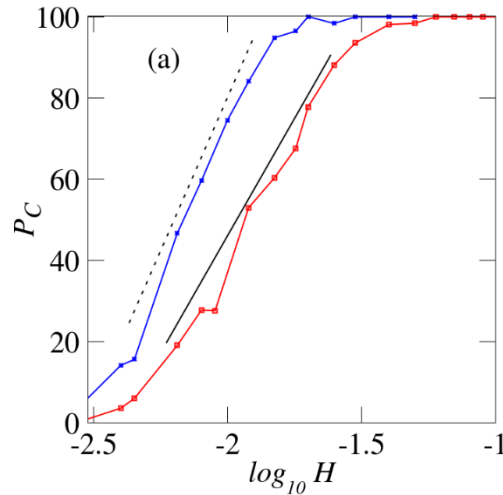
$$t = 10^5, 10^7, 10^9$$

Single site excitations, $L=1$, for $W=6$, $H=0.02$ [Senyange & S., Physica D (2022)].

The GALI_2 can identify chaos much more clearly than the MLE.

Decreasing nonlinearity

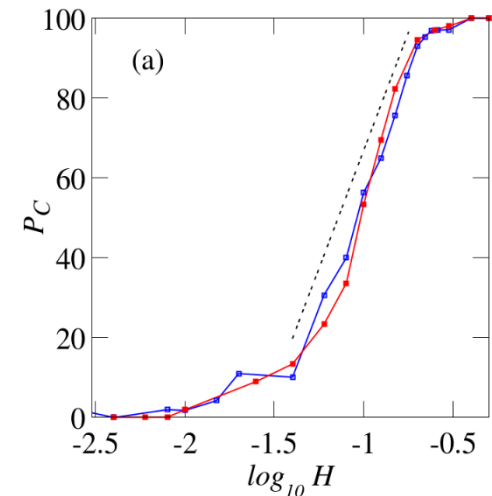
Single site excitations



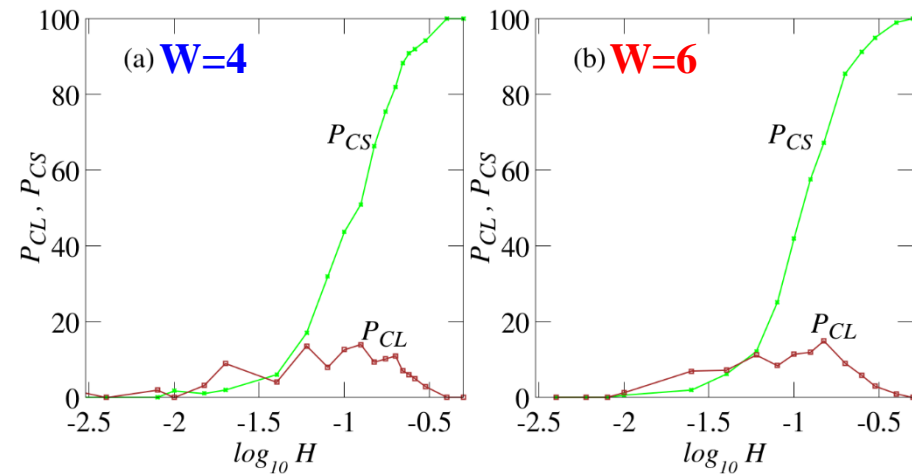
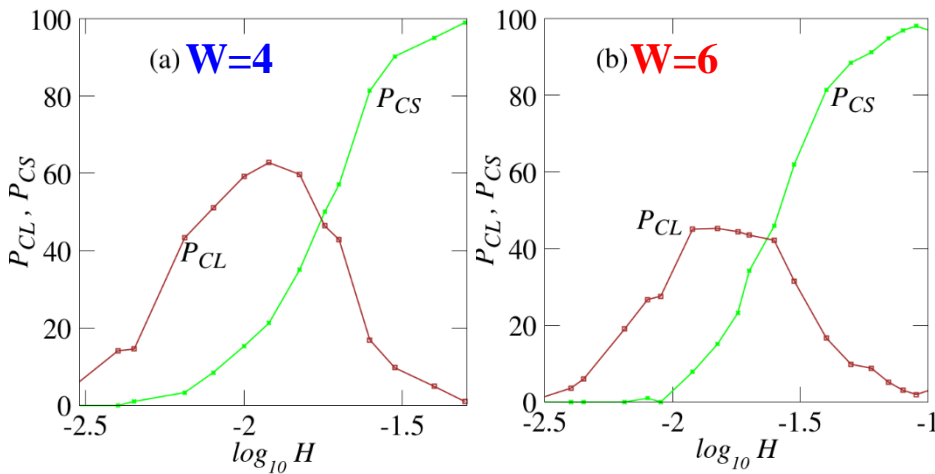
P_C : % of chaotic orbits

$W=4$, $W=6$

Single mode excitations



P_{CL} : % of localized chaos P_{CS} : % of spreading chaos



Energy thresholds for transition to regular motion and to spreading chaos are lower for single site excitations which permit mode interactions [Senyange & S., Physica D (2022)].

Summary

We investigated in depth the spatiotemporal chaotic behavior of the DKG multidimensional Hamiltonian system.

- Identification of 2 different dynamical spreading regimes: **weak and strong chaos**
- The MLE reveals the decrease of the system's chaoticity in time
Weak chaos: $\Lambda \propto t^{-0.25}$ - Strong chaos: $\Lambda \propto t^{-0.30}$
- The DVDs provide information about the propagation of chaos
Wandering of localized **chaotic hot spots** in the lattice's excited part homogenize chaos.
- FMA computations uncover the characteristics of chaos evolution
Chaotic behavior appears at the central regions of the wave packet, being more pronounced in the strong chaos case.
- The GALI method allows the detailed study of the system's behavior when it approaches its linear limit
Clear identification of chaos.
Efficient distinction between **localized and spreading chaos**.
Identification of **energy thresholds** leading to global chaotic spreading and to the total absence of chaos.

Main references

- S. (2001) J. Phys. A, 34, 10029
- S., Bountis, Antonopoulos (2007) Physica D, 231, 30
- S., Bountis, Antonopoulos (2008) Eur. Phys. J. Sp. Top., 165, 5
- Flach, Krimer, S. (2009) PRL, 102, 024101
- S., Flach (2010) PRE, 82, 016208
- Lptyeva, Bodyfelt, Krimer, S., Flach (2010) EPL, 91, 30001
- Bodyfelt, Lptyeva, S., Krimer, Flach (2011) PRE, 84, 016205
- S., Gkolas, Flach (2013) PRL, 111, 064101
- Senyange, Many Manda, S. (2018) PRE, 98, 052229
- Senyange, S. (2022) Physica D, 432, 133154
- S., Gerlach, Flach (2022) Int. J. Bifurc. Chaos, 32, 2250074

Support



University of Cape Town
University Research Committee, Conference Travel Grant

